Kolmogorov Turbulence and Information Dissipation in Molecular Communication

Mahmoud Abbaszadeh, Yu Huang, *Graduate Student Member, IEEE*, Peter J. Thomas, Miaowen Wen, *Senior Member, IEEE*, Fei Ji, *Member, IEEE*, and Weisi Guo, *Senior Member, IEEE*

***Abstract*—Waterborne chemical plumes are studied as a paradigm for representing a means for molecular communication in a macro-scale system. Results from the theory of fluid turbulence are applied and interpreted in the context of molecular communication to characterize the information cascade, the information dissipation rate and the critical length scale below which information modulated onto the plume can no longer be decoded. The results show that the information dissipation decreases with increasing Reynolds number and that there exists a theoretical potential for encoding smaller information structures at higher Reynolds numbers.**

***Index Terms*—Molecular communication, turbulence, Kolmogorov length-scale, energy cascade, information cascade.**

I. Introduction

MOLECULAR communication (MC) is concerned with information transfer by preserving information in the structure of chemical flow through molecular diffusion, advection or reaction [1]. Hence, the information transmission in MC is closely associated with the physics of fluid dynamics. The mechanism of MC, i.e., using chemical substances for information exchange, is prevalent in nature among organisms at various length scales, from intra-cell signaling [2] and bacterial communication [3] to airborne and waterborne pheromone signals [4]. A remarkable applications enabled by MC is targeted drug delivery that requires coordination and networking among nanomachines inside the body [5].

At nano-scale the physical conditions are such that the main mechanism of transport is mass diffusion [1]. Therefore fluid turbulence, for which other transport mechanisms are relevant, have hitherto hardly been considered at all in the context of MC. Nevertheless, MC is obviously not restricted to nano-scales, as demonstrated by insect and crustacean pheromone signaling [4]. Here turbulence does become a crucial issue affecting the reliability of the message transfer [6], [7]. The goal of the current study is to draw on turbulence theory to assess implications of relevance to MC at macro scale.

The conceptual framework for the theoretical description of fluid turbulence was defined by Kolmogorov [8], [9]. In the idealized scenario of homogeneous, isotropic turbulence - that is turbulence which is statistically invariant under translations and rotations, Kolmogorov's approach was based on Richardson's notion that larger eddies in a turbulent flow field are unstable and break up into successively smaller eddies. Thereby a cascade is created by which energy is transferred from the largest to the smallest length scales. The energy is eventually dissipated by the viscosity at a critical smallest length scale (see [10], [11]).

As indicated above, MC at macro-scale with turbulence is abundant in nature and technology (e.g., sensing contamination in underground water networks). In many such cases, these plumes carry a biological signal (e.g., communication mediated by pheromones [12]–[14]), and in others the chemical plume patterns are a proxy signal for a hazardous process (e.g., oil leakage [15] and source localisation [16], [17]).

If the information is embedded in the physical pattern of the plumes then the control of these chemical plumes becomes an essential aspect relevant to health and safety of marine life. This happens when the marine life communicate with chemical plumes, and any changes to the physical pattern of the plume can produce false alarm for recipient of the plume. Quantities such as the concentration amplitude level [18] and spatiotemporal characteristics [19]–[22] can be used for information encoding. The information modulated onto the chemical plume then propagates through the transmission channel and eventually arrives at the receiver side, where the proper signal detection schemes recover the transmitted information [23], [24].

In terms of fluid dynamics the chemical used to encode the information represents a passive scalar. That is a quantity which has no dynamic influence on the ambient turbulence

Manuscript received June 8, 2020; revised December 11, 2020; accepted February 7, 2021. Date of publication February 19, 2021; date of current version December 7, 2021. The work of Mahmoud Abbaszadeh, Peter J. Thomas, and Weisi Guo was supported by the U.S. AFOSR under Grant FA9550-17-1-0056. The work of Yu Huang, Miaowen Wen, and Fei Ji was supported in part by the National Natural Science Foundation of China under Grant 61871190, and in part by the China Scholarship Council under Grant 201906150032. The associate editor coordinating the review of this article and approving it for publication was J.-W. Choi. *(Corresponding author: Mahmoud Abbaszadeh.)*

Mahmoud Abbaszadeh is with the Department of Engineering and Physical Sciences, University of Southampton, Southampton SO17 1BJ, U.K. (e-mail: m.abbaszadeh@soton.ac.uk).

Yu Huang is with the School of Electronics and Information Engineering, South China University of Technology, Guangzhou 510641, China, and also with the School of Aerospace, Transport and Manufacturing, Cranfield University, Bedford MK43 0AL, U.K. (e-mail: ee06yuhuang@mail.scut.edu.cn).

Peter J. Thomas is with the School of Engineering, University of Warwick, Coventry CV4 7AL, U.K. (e-mail: p.j.thomas@warwick.ac.uk).

Miaowen Wen and Fei Ji are with the School of Electronics and Information Engineering, South China University of Technology, Guangzhou 510641, China (e-mail: eemwwen@scut.edu.cn; eefeiji@scut.edu.cn).

Weisi Guo is with the School of Aerospace, Transport and Manufacturing, Cranfield University, Bedford MK43 0AL, U.K. (e-mail: weisi.guo@cranfield.ac.uk).

Digital Object Identifier 10.1109/TMBMC.2021.3061037

2332-7804 © 2021 IEEE. Personal use is permitted, but republication/redistribution requires IEEE permission.
See https://www.ieee.org/publications/rights/index.html for more information.

Authorized licensed use limited to: University of Warwick. Downloaded on December 07,2021 at 09:00:51 UTC from IEEE Xplore. Restrictions apply.

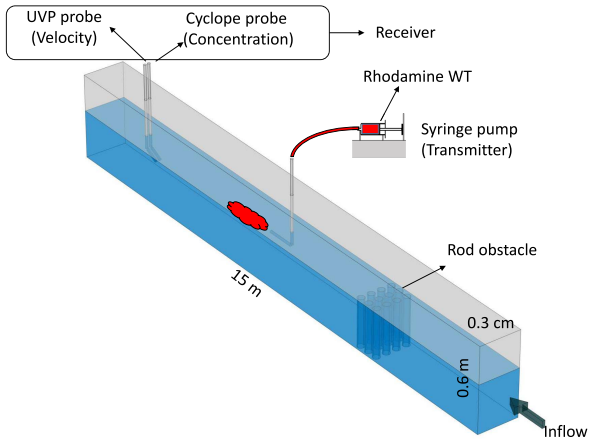

Fig. 1. Experimental arrangement in water channel (not to scale).

itself. The concentration of the chemical varies in space and time as it becomes mixed and distributed by the turbulent flow. From an information-theoretical point of view, the velocity field of the chemical plume contains a certain amount of information. This is so because the velocity field near the emitter of the plume is correlated to the velocity field some distance away [11], [25]–[27].

The goal here is to introduce established theoretical concepts for the energy cascade of turbulence and for the mixing of passive scalars, and apply these to chemical plumes as an example for a macro-scale MC system, interpreting the results from the viewpoint of information theory. The aim is to find the critical smallest length scale below which information modulated onto chemical plumes by means of a passive tracer can no longer be decoded and the rate at which information is dissipated.

II. Experimental Set Up

Experiments were conducted inside a water channel with overall length 15 m and height 0.6 m. The channel width is $w = 0.3$ m and its fill level during operation was $h = 0.34$ m. The experimental arrangement is schematically illustrated in Fig. 1. An obstacle consisting of an array of smooth steel rods, each of diameter 2.5 cm, can be placed 7 m downstream of the channel inlet as depicted in Fig. 1. When the water passes the obstacle then turbulence is generated in the wake of the rods.

It is assumed that the turbulence in the water channel is statistically steady when the obstacle is absent. The flow in the wake of the obstacle will be referred to as modified turbulence. Its statistical properties depend on the distance from the obstacle. This is so because sufficiently far downstream from the obstacle the flow will have resumed the properties of steady turbulence after all turbulent structures generated by the obstacle have been dissipated by the action of viscosity.

A syringe-pump arrangement is located 1 m downstream of the obstacle and acts as an information transmitter (Tx). The information is represented by defined amounts of fluorescent tracer (Rhodamine WT) which has an aqueous release concentration $C_0 = 10^5$ ppb. The tracer is injected sequentially into the channel by Tx. The release velocity (0.2 ms^{-1}) approximately matches the velocity of the ambient liquid to minimize biasing due to significant shear layers and additional turbulence resulting from the scalar release [28]. The released liquid quickly adopts the flow velocity of the ambient water and is then transported along as a passive scalar.

TABLE I
Experiment Parameters

Variable	Value
Channel dimensions	15 m $\times$0.6 m $\times$0.3 m
Distance between Tx and Rx, d	1 m to 5 m
Diameter of rods, D	25 mm
Schmidt number of Rhodamine WT, Sc	2100
Kinematic Viscosity of water, ν	1×10^{-6} m^2s^{-1}
Density of water, ρ	$1000\,\text{kgm}^{-3}$
Transmitter Concentration, C_0	10^5ppb
Mean velocity at level of Tx-Rx in steady turbulence, U_0	0.16, 0.23, 0.295 m s^{-1}

A receiver (Rx) is mounted at a distance in the range 1 m $\leq d \leq$ 5 m downstream of Tx. The receiver comprises an Ultrasonic Velocity Profiler (UVP) [29] combined with a CYCLOPS-7 Submersible Fluorometer [30] such that it can concurrently measure the flow velocity and the Rhodamine tracer concentration. The maximum axial extent of the section measurable with the UVP probe is 185 mm. The spatial and temporal measurement resolution of the velocity field is 0.74 mm and 63 ms, respectively. The temporal resolution of the CYCLOPE is 2 Hz and it measures the concentration at a single point along the channel.

Water was pumped through the channel at rates yielding mean flow velocities U_0 of 0.16, 0.23 and 0.295 ms^{-1} at the height level connecting Tx and Rx. A global Reynolds number to characterize the dynamics in the open channel flow is defined as $Re_0 = U_0 L/\nu$, where $L = A/P$ represents the hydraulic radius of the channel with its wetted cross-sectional area $A = wh$ and its wetted perimeter $p = 2h + w$ [31]. For the three values of the flow velocities U_0 for which experiments were conducted, this yields values Re_0 of 16,000 24,000 and 30,000.

The velocity component in the main flow direction inside the channel is measured as a function of time t and distance x from Rx and referred to by $u(t, x)$. The time-averaged mean flow velocity at any particular location in the flow field is denoted by u_0 and its associated fluctuating component is u'. Similarly the tracer concentration is $C(t, x)$ with random fluctuation (variance) $\langle C^2 \rangle$.

On-off keying (OOK) modulation [32], a special case of the binary concentration shift keying, is used for the tracer release at Tx. Note that in OOK, the transmission of bit '1' is represented by the emission of a chemical plume for a time period of t_p, while the bit '0' message corresponds to a period of no tracer release.

III. On-Off Key Dye Injection

A. Injection Mechanism

Single emissions and consecutive emissions are considered for OOK dye injection. In single emission, 10 ml of fluorescent

Authorized licensed use limited to: University of Warwick. Downloaded on December 07,2021 at 09:00:51 UTC from IEEE Xplore. Restrictions apply.

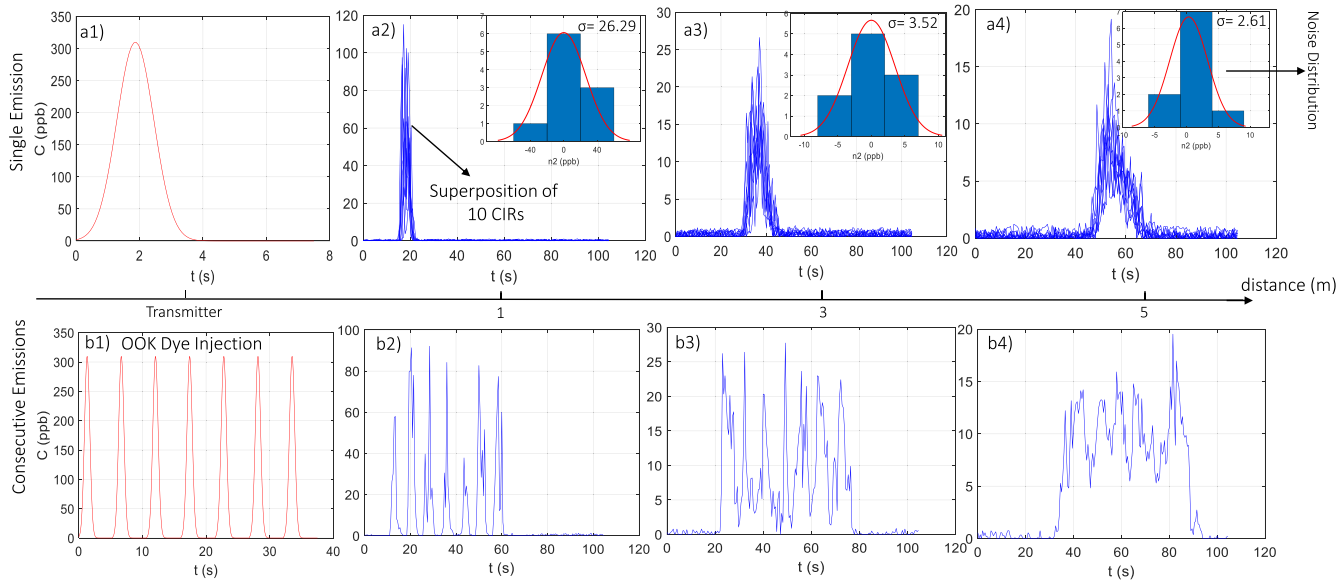

Fig. 2. a1) Concentration profile at $d = 1$ m from the transmitter. This profile is fitted by the Gaussian distribution to derive the OOK injector pulse function. The inset shows histogram of the peak values of the concentration profiles at $d = 1$ m from the transmitter. Superposition of ten CIRs at a2) $d = 1$ m, a3) $d = 3$ m a4) $d = 5$ m. b1) Seven consecutive signals sent to the channel by the transmitter. Seven consecutive signals received by the receiver at b2) $d = 1$ m, b3) $d = 3$ m b4) $d = 5$ m.

tracer liquid (the information carrier) is released into the channel for a period of $t = 2.5$ s. A perfect step-pulse release is unrealistic. Therefore the concentration profile in steady turbulence at a location 1 m downstream of the injector (transmitter) is considered as the release function [see Fig. 2(a1)] representing bit '1'. The superposition of 10 single emissions in 3 different locations downstream of the injector is displayed in Fig. 2(a2-a4). The distribution of the peak amplitudes at each location is displayed in the inset of each of Fig. 2(a2-a4). The figures reveal that the variance of the peak amplitudes decreases with distance from the transmitter. The consecutive-emission scenario is illustrated in Fig. 2(b1-b4). The symbol duration for each bit '1' is $t_p = 7.5$ s with time delay $\Delta t_p = 5.0$ s between each pair of successive puffs. At $d = 1.0$ m downstream of the transmitter, the individual bit '1' is distinguishable but as the distance from the transmitter increases, the effects of ISI on the received signal is intensified in a way that at $d = 5.0$ m a sophisticated detection algorithm is required to detect the received signal.

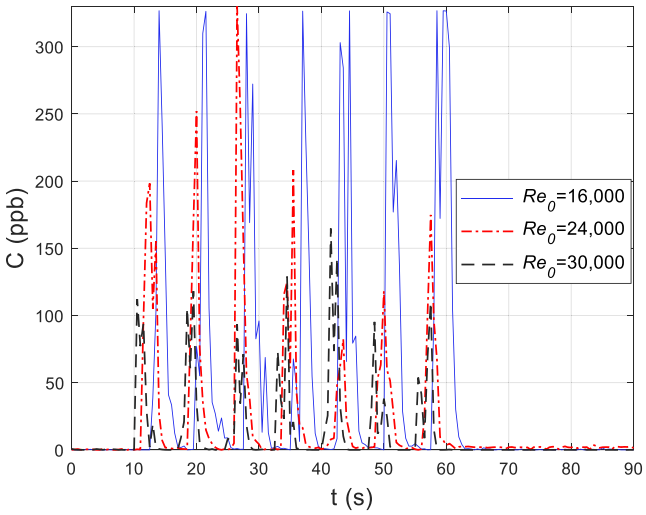

Fig. 3. Seven-bit signal sequences for the tracer concentration, for three different values of the Reynolds number Re_0, in steady turbulence.

B. Concentration Data

Figure 3 displays raw data for the concentration $C(t)$ recorded by the Fluorometer for the release of seven consecutive bit '1' symbols in steady turbulence. The Fluorometer was located $d = 1.0$ m downstream of Tx. Data for the three different release Reynolds numbers Re_0 are included.

Figure 3 shows that the information at higher Re_0 arrives at Rx earlier than those with lower Re_0 resulting from higher mean velocity U_0 at higher Re_0. The result to note from Fig. 3 is that the tracer concentration detected by the Fluorometer decreases substantially with increasing Reynolds number. This reflects increased turbulence levels and, associated, more effective mixing at higher Re_0. The significant reduction in the signal amplitude can degrade the so-called bit error rate (BER) performance. This is an important index characterizing the reliability of a communication system. It is defined as the ratio of incorrectly decoded bit number to the total transmitted bit number; such that lower BER values represent better performance.

Figure 4 compares measured concentration levels for the seven-bit sequence of Figure 3 at $Re_0 = 16,000$ for steady turbulence to a corresponding bit sequence for modified turbulence existing when the obstacle is in place. The figure reveals that the concentration levels for the modified turbulence are substantially lower than those for the steady turbulence. This signal attenuation implies that the turbulence generated by the obstacle has significantly increased the mixing efficiency. The

Authorized licensed use limited to: University of Warwick. Downloaded on December 07,2021 at 09:00:51 UTC from IEEE Xplore. Restrictions apply.

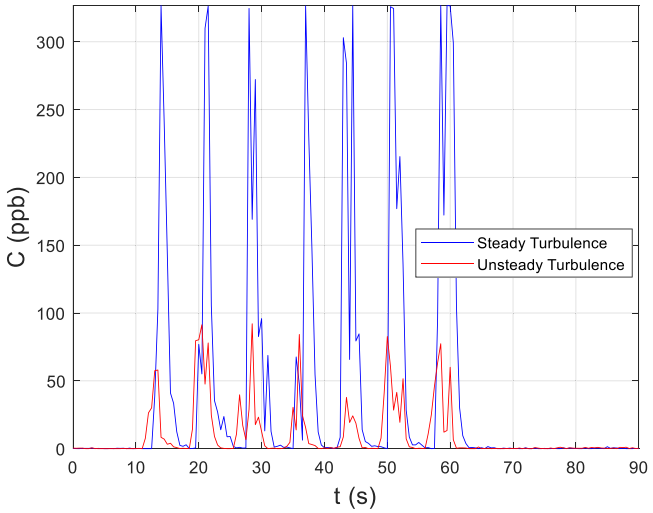

Fig. 4. Seven-bit signal sequences for the tracer concentration for steady turbulence at $Re_0 = 16,000$ in comparison to data for the corresponding flow in the modified turbulence.

measurements revealed that the obstacle leads to an almost tenfold increase of the turbulence level $\langle u'^2 \rangle$ in comparison to steady turbulence in the absence of the obstacle.

IV. Turbulent Velocity Signal

To quantify the different length scales of a turbulent flow the spatiotemporal variation of the velocity field is required. Figure 5 and Fig. 6 illustrate examples of such variations obtained from our experiments. Figure 5 displays the temporal variation of the flow velocity $u(t)$ at a point $d = 1.0$ m downstream of Tx. The random nature of the signal reflects that a wide range of frequencies associated with the hierarchy of tangled eddies of varying sizes are embedded in the turbulent flow. Lower frequency components are associated with large eddies and higher frequency components correspond to smaller eddies.

Whilst Fig. 5 illustrated temporal velocity fluctuation Fig. 6 shows a spatial velocity variation $u(x)$ of a flow section at a particular instance in time. The large-scale fluctuations in the lower plot of Fig. 6 qualitatively reflect the approximate scale of the largest eddies. A quantitative measure of this scale is defined in Section IV-A.

A. Velocity Correlation and Integral Length Scale

The correlation function is one main tool for analyzing velocity data in fluid turbulence. It can be used to assess the distance required between sample points in the flow field for the velocity values to become effectively uncorrelated. The velocity correlation is given by the ensemble average [11]

$$R_{xx} = \frac{1}{2X} \int_{-X}^{X} u'(x)u'(x+r)dr = \langle u'(x)u'(x+r) \rangle. \quad (1)$$

The associated longitudinal velocity correlation function is a dimensionless component of R_{xx} given by [11]

$$f(r) = \frac{R_{xx}(r)}{R_{xx}(r=0)} \quad (2)$$

and satisfying $f(r = 0) = 1$.

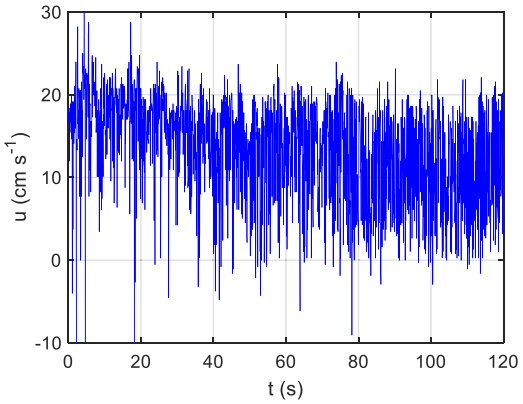

Fig. 5. Temporal variation of velocity, $u(t)$ at $d = 1$ m from Tx.

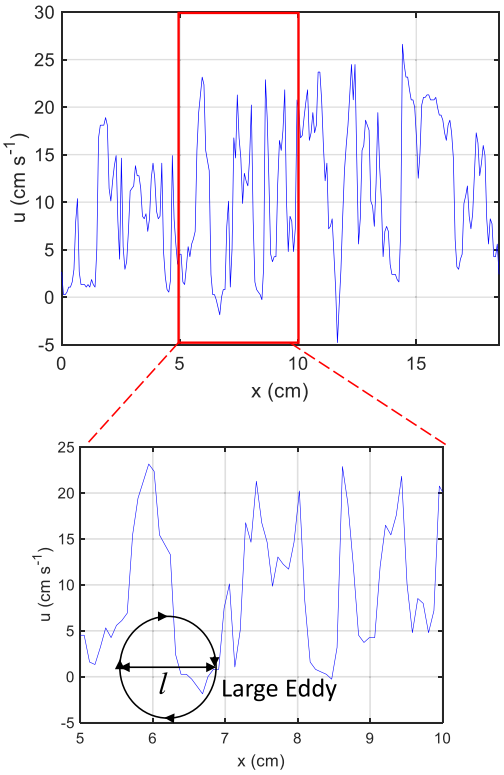

Fig. 6. Spatial variation of velocity, $u(x)$ over a section extending 185 mm upstream of Rx, which itself was located $d = 1$ m downstream of Tx.

The integral scale l characterizes the extent of the region where velocities are appreciably correlated. It represents the length scale of the largest eddies containing most of the energy (see Fig. 6) and it is given by [11]

$$l = \int_0^{\infty} f(r)dx. \quad (3)$$

B. Energy Cascade

According to the Wiener–Khinchin theorem [33] the Fourier transform $\mathfrak{F}$ of the autocorrelation function R_{xx} of (1) yields the one-dimensional energy spectrum $E(k)$ of u'

$$\mathfrak{F}[R_{xx}] = 2\pi |U(k)|^2 = E(k) \quad (4)$$

Authorized licensed use limited to: University of Warwick. Downloaded on December 07,2021 at 09:00:51 UTC from IEEE Xplore. Restrictions apply.

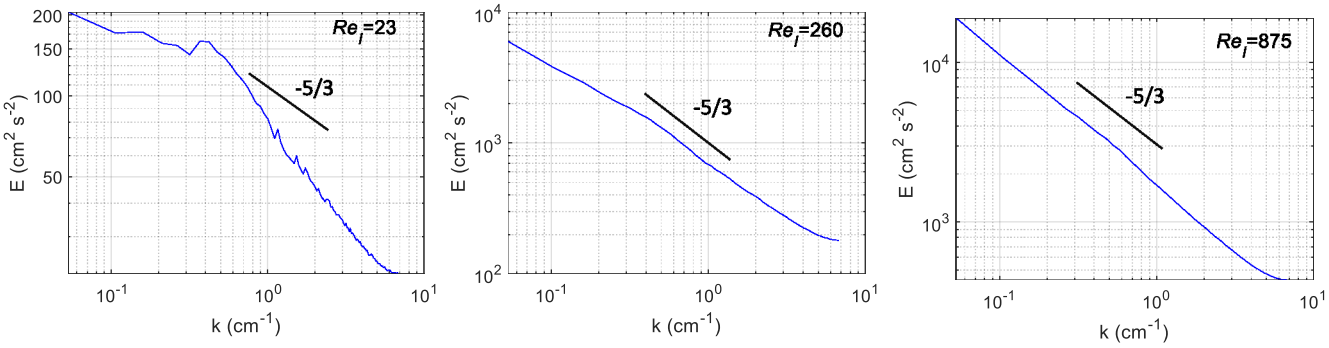

Fig. 7. Energy spectrum for three different values of the Reynolds number Re_l of the large eddies.

where $U(k) = \mathfrak{F}(u')$ is the Fourier transform of u' and k is the wavenumber.

Figure 7 displays the energy spectrum of the velocity field as a function of the wavenumber k. Data are shown for three different values of a large-scale Reynolds number defined as $Re_l = lu_l/\nu$. Here u_l is velocity of the largest eddies for which estimates can be inferred from the measured UVP data. The figure reveals that the data approach $E \propto k^{-5/3}$ for increasing Re_l. To readers unfamiliar with fluid dynamics we highlight that this relation between E and k, at high Reynolds number, represents one of the most celebrated results in turbulence and is referred to as the Kolmogorov five-thirds law [10]. The fact that the $-5/3$ dependence is obtained for the present measurements gives us confidence in our UVP velocity data.

While the integral scale of (3) represents the measurable scale of the largest eddies the size of the smallest eddies, η, and their associated velocity u_η cannot be resolved experimentally; they have to be obtained from theoretical consideration. A Reynolds number associated with these two quantities is defined as $Re_\eta = \eta u_\eta/\nu$.

It is known (see [11]) that most eddies break up on a time scale of their turn-over time. For the largest eddies this time scale is l/u_l. Therefore the rate at which energy (per unit mass) is transferred down the energy cascade from the largest eddies is [11]

$$\epsilon_l = \frac{u_l^2}{l/u_l}. \tag{5}$$

The energy cascade comes to a halt at small scales where the viscous forces are dominant and Re_η will be of order unity. The rate of dissipation of energy at the smallest scales is given by (see [11]),

$$\epsilon_\eta = \nu \frac{u_\eta^2}{\eta^2} \tag{6}$$

When the turbulent flow is statistically steady, the rate of the generation and dissipation of energy at large and small scales are the same. If this were not the case, then energy would accumulate at an intermediate scale. From (5) and (6) it therefore follows that

$$\frac{u_l^3}{l} \sim \nu \frac{u_\eta^2}{\eta^2}. \tag{7}$$

The Reynolds number $Re_\eta = \eta u_\eta/\nu$ at smallest scales, where viscous forces dominate, must be of order unity. Rearranging (7) by considering $Re_\eta \sim 1$ yields

$$\eta \sim l Re_l^{-3/4}. \tag{8}$$

The expression in (8) provides a means to quantify the smallest scale η of the turbulent energy cascade based on the known size l of the largest eddies and their associated Reynolds number Re_l. The length scale η and the velocity scale u_η are referred to as the Kolmogorov microscales [11].

V. Results and Discussion

A. Information Length Scale

Analogous to the Kolmogorov microscale η for turbulence, one can define a characteristic length scale, η_c, for the molecular information. When the length scale of the eddies is smaller than η_c, the propagation of the information molecules is dominated by diffusion. The kinetic energy of the molecules is small and the Reynolds number Re_η is of order unity. Therefore inertial effects are negligible and viscous forces cause dissipation of energy.

The length scales η and η_c are related by the Schmidt number (see [11]). This non-dimensional number is defined as $Sc = \nu/\alpha$ and characterizes the ratio of momentum diffusivity, ν, and mass diffusivity, α. When $\nu > \alpha$ then vorticity diffusion is more effective than the diffusion of C and vice versa.

For the current experiments with Rhodamine in water the data of [34] provide $Sc \sim 2100$. This value implies that the diffusion of vorticity is substantially more effective than mass diffusivity. Therefore it is expected that a fine-scale structure of the concentration will develop such that $\eta_c < \eta$.

For high Schmidt number, η and η_c are related by [11]

$$\eta_c \sim \eta \left(\frac{\alpha}{\nu}\right)^{1/2}. \tag{9}$$

Thus, for $Sc = 2100$ one has $\eta_c/\eta \approx 0.02$. The range between η_c and η is referred to as the viscous-convective subrange in [11]. From (8) and (9) one finds for the current study where $Re_l = 23, 260, 875$ that $\eta_c = 0.011$, 0.0084, 0.0049 mm, respectively. Thus, η_c decreases with increasing Re_l. This implies that, theoretically, smaller information

Authorized licensed use limited to: University of Warwick. Downloaded on December 07,2021 at 09:00:51 UTC from IEEE Xplore. Restrictions apply.

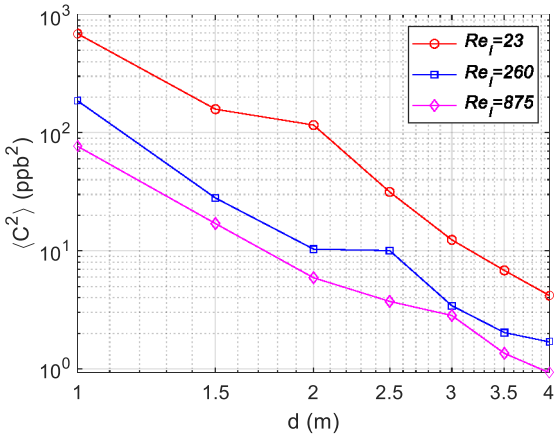

Fig. 8. Variation of $\langle C^2 \rangle$ of the molecular signals with distance d from Tx for three different values of the Reynolds number Re_l for modified turbulence.

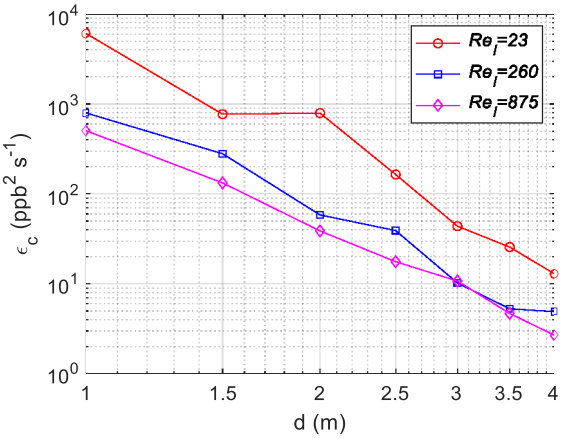

Fig. 9. Variation of information dissipation rate ϵ_c of the molecular signals with distance d from Tx for three different values of the Reynolds number Re_l for modified turbulence.

structures can be embedded in flows at higher Reynolds numbers.

In the context of MC the main implication of these considerations is that η_c is the theoretical smallest scale for which messages from a molecular signal concentration can be decoded. For values that lie below the diffusion-dominated scale η_c, it will no longer be possible to recover the original signal.

B. Information Dissipation Rate

In the preceding section η_c is the transition length scale between the energy containing and diffusion-dominated length scales. As is discussed in [11] the quantity arises from considerations that suggest that the energy cascade resulting in the energy dissipation rate of (5) should be accompanied by a corresponding cascade of $\langle C^2 \rangle$. The discussions conclude that when the same mechanism is used to create the turbulence and the scalar fluctuations, as is the case in our experiments, then the flux of scalar $\langle C^2 \rangle$, can be estimated by [11]

$$\epsilon_c \sim \frac{\langle C^2 \rangle}{l/u}. \tag{10}$$

The expression in (10) warrants a comment. In conventional diffusion-based MC, at nano scales, the variations of the concentration $\langle C^2 \rangle$ is ordinarily regarded as resulting from random noise with constant probability distribution [1], [35]. Similarly, in steady homogeneous isotropic turbulence the statistics of the noise of the channel would not change with location such that $\langle C^2 \rangle$ would also remain constant. However, in the presence of a disturbance-generating device, such as the turbulence-generating obstacle in Fig. 1, the variance $\langle C^2 \rangle$ is modified according to the particular characteristics of the device in place and, therefore, $\langle C^2 \rangle$ changes with the spatial separation from the device. Thus, the device-specific modifications of $\langle C^2 \rangle$ become an inherent part of the MC channel. Figure 8 displays the decrease of $\langle C^2 \rangle$ as a function of the distance d from Tx in the downstream flow field of the obstacle for three different values of Re_l. The figure also reveals that, in the present case one has, approximately, $\langle C^2 \rangle \propto d^{-3.3}$.

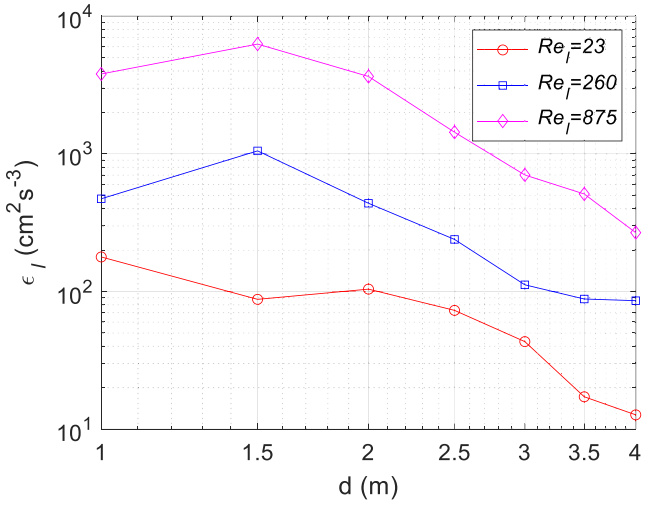

Fig. 10. Energy dissipation rate, ϵ_l vs. distance from transmitter.

Similar to (5), the information dissipation rate ϵ_c of (10) is calculated using the length scale l and the velocity scale u for the largest eddies which can be inferred from signals measured by the UVP probe (see Fig. 6). Figure 9 displays ϵ_c as a function of the distance d for three different values of the Reynolds number Re_l.

The figure reveals two results. Firstly, the information dissipation rate decreases with increasing distance d from Tx. This means that, as the information carrying tracer gets diluted to successively lower concentrations the rate at which it dilutes further must decrease. Secondly, at any particular distance d the information dissipation rate also decreases with increasing Re_l.

For comparison to ϵ_c of Figure 9 the energy dissipation rate ϵ_l from (5) is displayed in a corresponding plot in Fig. 10. Figure 10 shows that ϵ_l also decreases with increasing distance d. Most importantly, however, the figure reveals that, contrary to ϵ_c, for any particular distance d the value of ϵ_l increases with Re_l.

The result that the information dissipation rate ϵ_c decreases with increasing Re_l may appear counter intuitive because

Authorized licensed use limited to: University of Warwick. Downloaded on December 07,2021 at 09:00:51 UTC from IEEE Xplore. Restrictions apply.

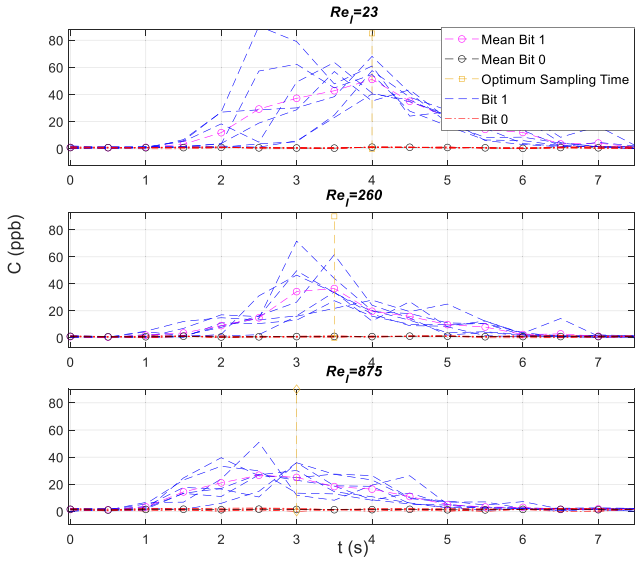

Fig. 11. Superposition of temporal concentration variations for seven individual bit '1' and bit '0' signals in modified turbulence and their associated respective mean curves for three different values of the Reynolds number Re_l ($d = 1.5$ m).

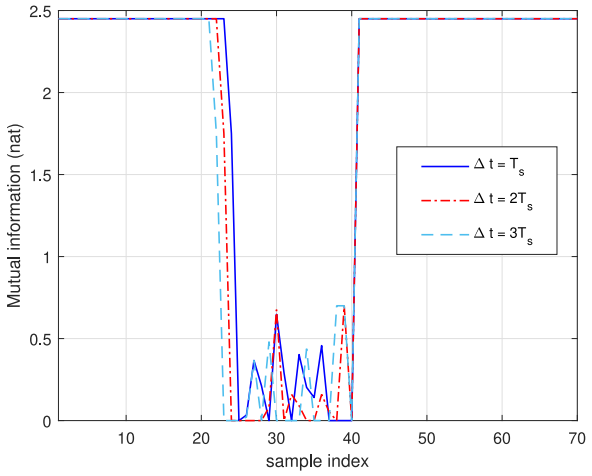

Fig. 12. $I(X_1; X_2)$ with various Δt.

stronger turbulence levels at higher Reynolds numbers have increased energy dissipation rates. However, increased turbulence leads to more efficient scalar mixing and, therewith, the power of the molecular signal quickly reduces to low levels. Accordingly the information dissipation rate necessarily reduces due to the remaining low information content available.

This issue is illustrated in Fig. 11. The figure shows the superposition of seven individual bit '1' and bit '0' signals together with their associated respective mean curves in the modified turbulence. The figure illustrates that the information amplitude has reduced to low levels for the highest value of Re_l.

In summary, the issues of turbulence and mixing of passive scalars are of fundamental relevance to macroscale MC systems. From the viewpoint of information theory, it is important to understand that the energy cascade and the associated information cascade are interrelated and they cannot be examined separately.

C. Mutual Information

In the current context, the transmitted signal is represented by the concentration of ejected fluorescent liquid, and the corresponding received signal is the concentration at the receiver with the unsteady turbulence background. Conventionally, the mutual information between the scalar input and output random variables *X* and *Y* are considered in molecular communication [36], and it quantifies the uncertainty reduction of the random variable *X* or *Y*, given the observation of another one. In this case, the mutual information is given by

$$\begin{aligned} I(X;Y) &= H(X) - H(X|Y) = H(Y) - H(Y|X) \\ &= \sum_x \sum_y P(X=x, Y=y) \\ &\quad \times \log \frac{P(X=x, Y=y)}{P(X=x)P(Y=y)}, \end{aligned} \tag{11}$$

where $H(\cdot)$ is the entropy function, and $P(\cdot)$ represents the probability. Note that the probability distribution functions are required to obtain the analytical mutual information.

To avoid the strong turbulence effect in the near field, the concentration value with steady turbulence at $d = 1$ m can be sampled as the transmitted signal. In each realization, the transmitted concentration signal has a sharply rising trend to reach its peak at the first stage, and it then undergoes a rapid decline.

Since there are multiple samples of the transmitted signal, we may further consider the mutual information between the *n*-dimensional random vector $(X_1, X_2, \ldots, X_n)$ and random variable *Y*. To find the dependency between the samples of the transmitted signal at different times, mutual information can be used as the metric [37]. Without loss of generality, we consider $I(X_1, X_2)$, where X_1 and X_2 are the observation random variable sampled at t_1 and t_2, and their time difference is defined by

$$\Delta t = |t_2 - t_1| = nT_s, \tag{12}$$

where *n* is an integer, and T_s represents the sampling period. Due to the absence of probability density functions, we resort to Kraskov's method, which provides a way for mutual information estimation that only requires the data set of random variables [38]. In light of this, the roughly estimated mutual information between the samples that has various time difference is shown in Fig. 12. Intuitively, the neighbor samples have strong dependency.

By using the chain rule [39], we have

$$I(X_1, X_2, \ldots, X_n; Y) = \sum_{i=1}^{n-1} I(X_i; Y|X_1, X_2, \ldots, X_{i-1}). \tag{13}$$

Hence, compared with (11), one may obtain higher mutual information by using the random vector as input instead of the scalar random variable. Yet, its computation requires more

Authorized licensed use limited to: University of Warwick. Downloaded on December 07,2021 at 09:00:51 UTC from IEEE Xplore. Restrictions apply.

probability distribution functions, making the analytical results hard to obtain.

VI. Conclusion and Future Works

Waterborne chemical plumes were studied as a paradigm for a means of MC at macro scales. In experiments information was modulated onto chemical plumes represented by means of pulse sequences of a fluorescent tracer. As fluid turbulence mixes the tracer with the ambient carrier fluid and spatiotemporal concentration fluctuations are established in the flow field whose development is governed by the background turbulence field.

Results from the theory of fluid turbulence describing the turbulent energy cascade were applied and interpreted in terms of a corresponding information cascade associated with the mixing of the tracer. This enabled characterizing the theoretical critical information micro-scale below which information modulated onto the plume can no longer be decoded. This scale decreases with increasing turbulence which implies a theoretical potential for encoding smaller information structures at higher Reynolds number. Moreover, the information dissipation rate was found to decrease for the increased turbulence levels at higher Reynolds number. The latter result arising due to more efficient mixing at higher Reynolds numbers which decreases the remaining power of the molecular signal. Finally, the analytical mutual information had been defined, while the more accurate results will be considered in our future work.

References

[1] T. Nakano, A. W. Eckford, and T. Haraguchi, *Molecular Communication*. Cambridge, U.K.: Cambridge Univ. Press, 2013.

[2] T. Nakano *et al.*, "Random cell motion enhances the capacity of cell-cell communication," *IEEE Trans. Mol. Biol. Multi-Scale Commun.*, vol. 5, no. 2, pp. 158–162, Nov. 2019.

[3] L. C. Cobo and I. F. Akyildiz, "Bacteria-based communication in nanonetworks," *Nano Commun. Netw.*, vol. 1, no. 4, pp. 244–256, Dec. 2010.

[4] T. Wyatt, *Pheromones and Animal Behavior: Chemical Signals and Signatures*, 2nd ed. Cambridge, U.K.: Cambridge Univ. Press, 2014.

[5] N. Farsad, H. B. Yilmaz, A. Eckford, C.-B. Chae, and W. Guo, "A comprehensive survey of recent advancements in molecular communication," *IEEE Commun. Surveys Tuts.*, vol. 18, no. 3, pp. 1887–1919, 3rd Quart., 2016.

[6] B. D. Unluturk and I. F. Akyildiz, "An end-to-end model of plant pheromone channel for long range molecular communication," *IEEE Trans. Nanobiosci.*, vol. 16, no. 1, pp. 11–20, Jan. 2017.

[7] M. Abbaszadeh, I. U. Atthanayake, P. J. Thomas, and W. Guo, "Molecular signal tracking and detection methods in fluid dynamic channels," *IEEE Trans. Mol. Biol. Multi-Scale Commun.*, vol. 6, no. 2, pp. 151–159, Nov. 2020.

[8] A. N. Kolmogorov, "The local structure of turbulence in incompressible viscous fluid for very large Reynolds numbers," *Doklady Akademiia Nauk SSSR*, vol. 30, pp. 301–305, Jul. 1991.

[9] A. N. Kolmogorov, "On degeneration (decay) of isotropic turbulence in an incompressible viscous liquid," *Doklady Akademiia Nauk SSSR*, vol. 31, pp. 538–540, Jul. 1941.

[10] S. B. Pope, *Turbulent Flows*. Bristol, U.K.: IOP Publ., 2001.

[11] P. A. Davidson, *Turbulence: An Introduction for Scientists and Engineers*. Oxford, U.K.: Oxford Univ. Press, 2015.

[12] M. J. Weissburg, "Waterborne chemical communication: Stimulus dispersal dynamics and orientation strategies in crustaceans," in *Chemical Communication in Crustaceans*. New York, NY, USA: Springer, 2010, pp. 63–83.

[13] T. Breithaupt and M. Thiel, *Chemical Communication in Crustaceans*. New York, NY, USA: Springer, 2010.

[14] M. J. Weissburg *et al.*, "A multidisciplinary study of spatial and temporal scales containing information in turbulent chemical plume tracking," *Environ. Fluid Mech.*, vol. 2, nos. 1–2, pp. 65–94, Jun. 2002.

[15] Z. Lu *et al.*, "Microbial gene functions enriched in the deepwater horizon deep-sea oil plume," *ISME J.*, vol. 6, no. 2, pp. 451–460, Feb. 2012.

[16] W. Naeem, R. Sutton, and J. Chudley, "Chemical plume tracing and odour source localisation by autonomous vehicles," *J. Navig.*, vol. 60, no. 2, pp. 173–190, May 2007.

[17] S. Pang and J. A. Farrell, "Chemical plume source localization," *IEEE Trans. Syst., Man, Cybern. B, Cybern.* , vol. 36, no. 5, pp. 1068–1080, Oct. 2006.

[18] M. S. Kuran, H. B. Yilmaz, T. Tugcu, and I. F. Akyildiz, "Modulation techniques for communication via diffusion in nanonetworks," in *Proc. IEEE Int. Conf. Commun. (ICC)*, Kyoto, Japan, Jun. 2011, pp. 1–5.

[19] Y. Huang, M. Wen, L. L. Yang, C. Chae, and F. Ji, "Spatial modulation for molecular communication," *IEEE Trans. Nanobiosci.*, vol. 18, no. 3, pp. 381–395, Jul. 2019.

[20] Y. Huang, M. Wen, L.-L. Yang, C.-B. Chae, X. Chen, and Y. Tang, "Space shift keying for molecular communication: Theory and experiment," in *Proc. IEEE Global Commun. Conf. (GLOBECOM)*, Waikoloa, HI, USA, Dec. 2019, pp. 1–6.

[21] M. Ozmen, E. Kennedy, J. Rose, P. Shakya, J. K. Rosenstein, and C. Rose, "High speed chemical vapor communication using photoionization detectors," in *Proc. IEEE Global Commun. Conf. (GLOBECOM)*, Abu Dhabi, United Arab Emirates, Dec. 2018, pp. 1–6.

[22] E. Kennedy, P. Shakya, M. Ozmen, C. Rose, and J. Rosenstein, "Spatiotemporal information preservation in turbulent vapor plumes," *Appl. Phys. Lett.*, vol. 112, no. 26, pp. 666–697, Jun. 2018.

[23] I. Llatser, A. Cabellos-Aparicio, M. Pierobon, and E. Alarcón, "Detection techniques for diffusion-based molecular communication," *IEEE J. Sel. Areas Commun.*, vol. 31, no. 12, pp. 726–734, Dec. 2013.

[24] L. Khaloopour *et al.*, "An experimental platform for macro-scale fluidic medium molecular communication," *IEEE Trans. Mol. Biol. Multi-Scale Commun.*, vol. 5, no. 3, pp. 163–175, Dec. 2019.

[25] R. Cerbus and W. Goldburg, "Information content of turbulence," *Phys. Rev. E*, vol. 88, no. 5, Nov. 2013, Art. no. 053012.

[26] C. Granero-Belinchon, S. G. Roux, and N. B. Garnier, "Scaling of information in turbulence," *Europhys. Lett.*, vol. 115, no. 5, Sep. 2016, Art. no. 58003.

[27] I. Atthanayake, S. Esfahani, P. Denissenko, I. Guymer, P. J. Thomas, and W. Guo, "Experimental molecular communications in obstacle rich fluids," in *Proc. ACM Int. Conf. Nanoscale Comput. Commun.*, Reykjavik, Iceland, Sep. 2018, pp. 1–2.

[28] K. M. Talluru, J. Philip, and K. A. Chauhan, "Local transport of passive scalar released from a point source in a turbulent boundary layer," *J. Fluid Mech.*, vol. 846, pp. 292–317, Jul. 2018.

[29] R. Kotzé, J. Wiklund, R. Haldenwang, and V. Fester, "Measurement and analysis of flow behaviour in complex geometries using the ultrasonic velocity profiling (UVP) technique," *Flow Meas. Instrum.*, vol. 22, no. 2, pp. 110–119, Apr. 2011.

[30] (2010). *Cyclops-7 Submersible Sensors*. [Online]. Available: www.turnerdesigns.com

[31] R. Jeppson, *Open Channel Flow: Numerical Methods and Computer Applications*. Boca Raton, FL, USA: CRC Press, 2010.

[32] L. Shi and L.-L. Yang, "Error performance analysis of diffusive molecular communication systems with on-off keying modulation," *IEEE Trans. Mol. Biol. Multi-Scale Commun.*, vol. 3, no. 4, pp. 224–238, Dec. 2017.

[33] C. Chatfield, *The Analysis of Time Series: An Introduction*, 6th ed. Boca Raton, FL, USA: CRC Press, 2004.

[34] C. T. Culbertson, S. C. Jacobson, and J. M. Ramsey, "Diffusion coefficient measurements in microfluidic devices," *Talanta*, vol. 56, no. 2, pp. 365–373, Feb. 2002.

[35] M. Abbaszadeh *et al.*, "Mutual information and noise distributions of molecular signals using laser induced fluorescence," in *Proc. IEEE Global Commun. Conf. (GLOBECOM)*, Waikoloa, HI, USA, Dec. 2019, pp. 1–6.

[36] L. Lin, Q. Wu, F. Liu, and H. Yan, "Mutual information and maximum achievable rate for mobile molecular communication systems," *IEEE Trans. Nanobiosci.*, vol. 17, no. 4, pp. 507–517, Oct. 2018.

[37] A. Noel, K. C. Cheung, and R. Schober, "Optimal receiver design for diffusive molecular communication with flow and additive noise," *IEEE Trans. Nanobiosci.*, vol. 13, no. 3, pp. 350–362, Sep. 2014.

[38] A. Kraskov, H. Stögbauer, and P. Grassberger, "Estimating mutual information," *Phys. Rev. E, Stat. Phys. Plasmas Fluids Relat. Interdiscip. Topics*, vol. 69, no. 6, 2004, Art. no. 066138.

[39] T. M. Cover and J. A. Thomas, *Elements of Information Theory*. New York, NY, USA: Wiley, 2006.

Authorized licensed use limited to: University of Warwick. Downloaded on December 07,2021 at 09:00:51 UTC from IEEE Xplore. Restrictions apply.

Mahmoud Abbaszadeh received the B.S. degree in mechanical engineering, heat, and fluids, and the M.Sc. degree in mechanical engineering and energy conversion from the University of Kashan, Iran, in 2013 and 2015, respectively. He is currently pursuing the Ph.D. degree with the University of Warwick, to investigate molecular communication in turbulent fluid environments. He is a Research Fellow in environmental fluid mechanics with the University of Southampton. During his master's studies, he focused on CFD modeling of nanofluid heat transfer in cavities and microchannels. He applied the concept of Shannon capacity in the context of modulated information in turbulent chemical plumes. In November 2020, he joined the Water Engineering Group, University of Southampton as a Research Fellow. He is currently working on optimizing the design of algae raceway ponds in order to improve the mixing processes, gas transfer at gas–liquid interface, and carbon footprint reduction.

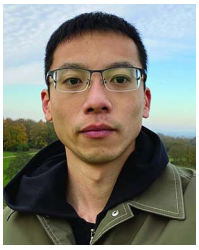

Yu Huang (Graduate Student Member, IEEE) received the B.S. degree in communication engineering from the Harbin University of Science and Technology, Harbin, China, in 2016. He is currently pursuing the Ph.D. degree in information and communication engineering with the South China University of Technology, Guangzhou, China. From 2018 to 2019, he was a visiting student of molecular communication with Yonsei University, Seoul, South Korea. Since January 2020, he has been visiting Cranfield University, Bedford, U.K., for emerging communication techniques. His main research interests include molecular communications and wireless communications. He was the winner of the Data Bakeoff Competition (Molecular MIMO) at the IEEE Communication Theory Workshop, Selfoss, Iceland, in 2019.

Peter J. Thomas received the Dipl.-Phys. and Dr.rer.nat. degrees in physics from Georg-August-Universität, Göttingen, Germany, in 1988 and 1991, respectively. Before joining the University of Warwick in 1995, he worked in Göttingen, with the Max-Planck Institute of Fluid Mechanics and Applied Mechanics and then with the German Aerospace Centre (DLR). He moved to the U.K. in 1992, for a post with the Department of Applied Mathematics and Theoretical Physics, University of Cambridge. In 2008, he was promoted to a Professor with the University of Warwick, where he is the Director of Fluid Dynamics Research Centre. His current research interests include the experimental and theoretical investigations of problems in fluid dynamics and of nonlinear mechanical processes in general. He received the International Union of Applied and Theoretical Mechanics Bureau Prize in 1996. He is a member of the European Mechanics Society.

Miaowen Wen (Senior Member, IEEE) received the Ph.D. degree from Peking University, Beijing, China, in 2014. From 2012 to 2013, he was a Visiting Student Research Collaborator with Princeton University, Princeton, NJ, USA. He is currently an Associate Professor with the South China University of Technology, Guangzhou, China. He has published two books and more than 100 journal papers. His research interests include a variety of topics in the areas of wireless and molecular communications. He was a recipient of the IEEE Asia–Pacific Outstanding Young Researcher Award in 2020, and four Best Paper Awards from IEEE ITST 2012, IEEE ITSC 2014, IEEE ICNC 2016, and IEEE ICCT 2019. He was the Winner of the Data Bakeoff Competition (Molecular MIMO) at the IEEE Communication Theory Workshop 2019, Selfoss, Iceland. He served as a Guest Editor for the IEEE JOURNAL ON SELECTED AREAS IN COMMUNICATIONS and the IEEE JOURNAL OF SELECTED TOPICS IN SIGNAL PROCESSING. He is currently serving as an Editor for the IEEE TRANSACTIONS ON COMMUNICATIONS and the IEEE COMMUNICATIONS LETTERS, and a Guest Editor for the IEEE JOURNAL OF SELECTED TOPICS IN SIGNAL PROCESSING (Special Issue on Advanced Signal Processing for Local and Private 5G Networks).

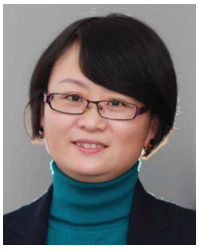

Fei Ji (Member, IEEE) received the B.S. degree in applied electronic technologies from Northwestern Polytechnical University, Xi'an, China, in 1992, and the M.S. degree in bioelectronics and the Ph.D. degree in circuits and systems from the South China University of Technology, Guangzhou, China, in 1995 and 1998, respectively. She was a Visiting Scholar with the University of Waterloo, Canada, from June 2009 to June 2010. She worked with the City University of Hong Kong as a Research Assistant from March 2001 to July 2002 and a Senior Research Associate from January 2005 to March 2005. She is currently a Professor with the School of Electronic and Information Engineering, South China University of Technology. Her research focuses on wireless communication systems and networking. She was the Registration Chair and the Technical Program Committee Member of IEEE 2008 International Conference on Communication System.

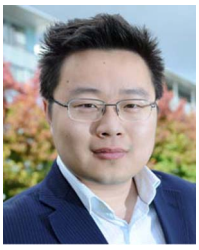

Weisi Guo (Senior Member, IEEE) received the M.Eng., M.A., and Ph.D. degrees from the University of Cambridge, U.K. He is the Chair Professor of Human Machine Intelligence with Cranfield University. He has published over 170 papers and is a PI on a number of molecular communication research grants. His research has won several international awards (IET Innovation 2015, Bell Labs Prize Finalist 2014, 2016, and 2019). He was a Turing Fellow of the Alan Turing Institute and is a Fellow of the Royal Statistical Society.

Authorized licensed use limited to: University of Warwick. Downloaded on December 07,2021 at 09:00:51 UTC from IEEE Xplore. Restrictions apply.